A High-Performance Standard Dipole Antenna Suitable for Antenna Calibration

Zhanghua Cai, *Student Member, IEEE*, Zibin Weng, *Senior Member*, *IEEE*, Yihong Qi, *Senior Member*, *IEEE*, Jun Fan, *Fellow*, *IEEE*, Weihua Zhuang, *Fellow*, *IEEE*

Abstract—**Ideal dipole antennas are desirable for antenna calibration. However, real-world implementation issues introduce inevitable non-ideal effects that can significantly affect the quality of calibration. In this communication, a 2-GHz standard dipole (SD) antenna is presented with an excellent overall performance. This result is achieved by an innovative design with an optimized element shape and an embedded (shielded) balun. The designed feeding structure is a balanced structure that transitions from parallel strip lines to coaxial lines. The feeding method avoids the impact of electromagnetic environment asymmetry while achieving an appropriate balance. The measured relative bandwidth of the dipole exceeds 15%, and the antenna gain is approximately 2 dBi. The cross-polarization ratio is greater than 27 dB in the horizontal plane, and the horizontal gain variation is less than 0.2 dB. The dipole has a symmetrical vertical plane pattern, and the maximum gain point does not deviate from the horizontal plane. The high performance of this SD makes it suitable for antenna calibration.**

Index Terms—**Standard dipole, antenna calibration, embedded balun, optimized element shape.**

I. Introduction

Tth gain of an antenna is a relative value. The gain value is given in units of dBi and is defined relative to an isotropic antenna. However, no isotropic antenna exists in reality. The typical gain value of a standard half-wave dipole can be obtained by numerical analysis methods, and the dipole is an antenna that can be made in practice. Therefore, the unit of dBd is often used as an alternative antenna gain unit in practical engineering, which is the gain defined relative to a standard dipole (SD). Moreover, dipole antennas have an omnidirectional pattern in the horizontal plane, which presents great advantages for calibrating multi-probe systems.

However, it is difficult to achieve ideal performance with an SD as this necessitates a complete balance in the practical design. The balance of an antenna is determined by the radiator, feeding structure, and electromagnetic (EM) environment. For a dipole, the radiator is symmetrical, and thus, the balance of the radiator can be easily ensured. However, difficulties lie in the balance of the feeding structure and EM environment.

The first difficulty is the balance of the feed. A coaxial cable is the most commonly used feeding component for an antenna. This approach provides an imbalanced feeding, and there exists a common-mode current on the outer surface of the outer conductor of the cable [1-3]. The generation of a common-mode current renders the current distribution on the dipole asymmetric, resulting in asymmetry in the radiation patterns and a change in efficiency. A balun is a structure that enables a conversion between balance and unbalance. According to its working principle, this balance can be divided into two basic types: current balance and voltage balance. To ensure a small gain variation in the horizontal plane, an SD generally adopts an end-fed mode instead of a side-fed mode. A current balun is commonly used for the end-fed structure. Typical methods include adding a metal choke balun [4-6] or ferrite beads [7, 8].
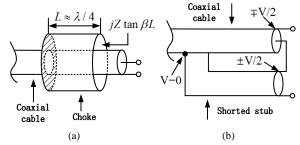

Fig. 1. (a) Current balun. (c) Voltage balun.

The choke balun is shown in Fig. 1(a). This balun suppresses the current by forming a high impedance through a metal choke. However, it is difficult to achieve the ideal high impedance in this way, and consequently, the effect of the choke is usually not sufficient. Because the length of the choke must be maintained near a quarter wavelength for the operating frequency, its bandwidth is usually less than 10%. Moreover, the dipole arm close to the coaxial line can be coupled with the choke, and a coupling current can form on the outer surface of the choke. As a result, SDs using choke baluns usually have the problem of asymmetry in the vertical pattern. Ferrite beads are generally effective only in the frequency band below 1 GHz, exhibiting a much weaker effect at higher frequencies [1]. In addition, ferrite

beads are associated with losses, which can reduce the measured radiated efficiency of the antenna [9]. Lastly, the suppression effect of ferrite beads on the common-mode current is limited, and thus, the antenna may still require a balun [8].

A voltage balun (the type III balun introduced in [10]) is shown in Fig. 1(b). A balanced structure, formed by the outer conductors, is achieved by adding a parallel shorted stub. Then, a zero voltage point is formed on the outer surface of the outer conductor at the junction to the added stub, thereby suppressing the common-mode current on the outer surface of the outer conductor from this junction to the rest of the feed cable. Compared with the choke balun, the voltage balun has a wider bandwidth and can better suppress the common-mode current. This type of balun is widely used in various antenna designs, such as loop antennas [3], directional dipoles [11, 12] and slot-loop antennas [13].

However, it is difficult to design a voltage balun for an SD because of the third factor that affects the antenna balance, that is, the balance of the EM environment. Due to the end-fed mode, the low level of radiation generated by the feeding structure will cause asymmetry in the vertical pattern. At the same time, the lower dipole arm will couple with the feeding structure, which can result in inconsistent radiation energy in the two arms and deteriorate the ripple. Therefore, when designing a voltage balun, the impact of EM environmental imbalance caused by the feeding structure should be minimized.

In summary, an SD should satisfy the three balances needed to achieve a close-to-ideal dipole pattern. For example, although the end-fed antennas described in [14, 15] have a symmetrical structure, they do not have a balun. Therefore, even if an ideal pattern can be obtained during simulation, the measured vertical plane patterns will produce large ripples and asymmetry due to the influence of the cable. The end-fed dipoles in [5, 16] have a metal sleeve structure, which can act as a choke; however, the structures are asymmetric, and the balun effect is limited. Thus, the measured patterns still generate ripples and asymmetry. [17, 18] used a voltage balun through a shorted stub. However, this structure will produce substantial EM environmental asymmetry at the center of the dipole, causing a current imbalance. Therefore, the patterns have obvious asymmetry, and the gain variation in the horizontal plane is large (approximately larger than 1 dB).

As far as we know, there have been no reports of SDs that can successfully achieve the three kinds of balance. To address this issue, an innovative embedded voltage balun is proposed in this communication. The balun realizes a balanced transition from parallel-strip lines to coaxial lines. This design avoids the influence on the central part of the dipole and reduces the influence of EM environmental asymmetry caused by the feed structure as much as possible by limiting the size of the wiring. In addition, the entire structure is placed inside a single dipole element. As a result, the voltage balun and the related feeding network are shielded and do not radiate, thus leaving the dipole pattern unchanged. Based on the innovative designs, a 2-GHz standard dipole is built, which demonstrates an overall performance better than almost all SDs reported in the literature or in the market, to the best of our knowledge.

The remainder of this communication is organized as follows. Section II introduces the design of the antenna and baluns. The simulated and measured results are provided in Section III. Finally, conclusions are drawn in Section IV.

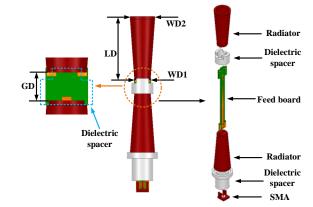## II. ANTENNA DESIGN

A. Antenna structure

Fig. 2. Antenna structure.

Fig. 2 shows the overall structure of the proposed dipole, which includes three main components: the radiator, the feeding substrate, and the dielectric spacer. A cone is used as the arm of the dipole. Compared with the traditional cylindrical dipole, a dipole with an inclination angle has the characteristics of a biconical antenna, which allows for a larger bandwidth. The cone shape can reduce coupling between the end of the dipole and the cable, reducing the asymmetry of the pattern caused by this coupling. However, the cone angle of the antenna cannot be too large. Otherwise, a large horizontal electric field component will be generated, resulting in deterioration of the cross-polarization ratio. This angle is optimized using simulations with a target relative bandwidth of 15% and a target cross-polarization ratio of 25 dB. The two dielectric spacers are composed of Teflon with a relative permittivity of 2.1.

Fig. 3(a) shows the stacking of the multilayer printed circuit board in which the embedded voltage balun and the related feeding network are constructed. The two core layers consist of Rogers 3003 material with a thickness of 0.508 mm and a relative permittivity of 3. The prepreg layer is an adhesive material (RO4450T) with a thickness of 0.101 mm and a relative permittivity of 3.3. The main part of the top conductor is used to connect the outer conductor of the coaxial cable and the lower radiator of the dipole. The middle layer is primarily used to connect the inner conductor of the coaxial cable and the upper radiator of the dipole. The bottom layer is mainly a parallel shorted stub, which forms a voltage balun. As shown in Fig. 3(b), the entire layout can be divided into five parts. Part 1 connects the board and the cones. The conductor pads in the dotted circles are solder joints. The details of the soldering connections are illustrated in Fig. 2. Part 2 contains a parallel-strip line. The two lines are respectively connected to the two cones, which are used for the transition between the radiators and the balun. Part

3 is the voltage balun. Because the current in the center of the dipole is strong, it has a great impact on the radiation performance. Thus, the balun is added after the parallel-strip line to avoid any impact on the center. The middle conductor is connected to the bottom stub at point A through a via-hole, and the top conductor is connected to the shorted stub at point C through via-holes. Part 4 connects the top layer and the bottom layer through two rows of via-holes to form a rectangular coaxial structure, which serves as a transition section between the balun input and the coaxial cable. Part 5 is the solder position for the subminiature version A (SMA) socket. The specific values of the parameters in Fig. 2 and Fig. 3(b) are in listed in Table I.
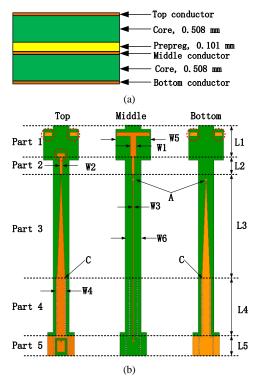

(a)

(b)

Fig. 3. Structure of the balun and related feeding network. (a) Board stackup. (b) Wiring layout.

TABLE I
GEOMETRIC PARAMETERS OF THE PROPOSED ANTENNA (UNIT: MM)

Parameter	Value	Parameter	Value	Parameter	Value
LD	33.5	L3	26.5	W3	0.1
WD1	8.5	L4	15.0	W4	2.6
WD2	13.2	L5	5.1	W5	8.9
L1	8.0	W1	1.5	W6	4.0
L2	4.6	W2	0.7	GD	5.1

B. Balun design

As shown in Fig. 4(a), the currents on the balanced transmission line have equal amplitude and opposite phase. When the transmission line is unbalanced, current asymmetry will arise. The current I_B on one path can be split into a differential-mode current I_{B_d} and the common-mode current I_{B_c}, as shown in Fig. 4(b). As shown in Fig. 4(c), the two conductors of the transmission line are connected by a shorted

stub, which introduces a current I_C. Because the structure and length of the shorted stub are the same as those for the path of I_{B_c}, the magnitudes of I_C and I_{B_c} are the same. Therefore, the two currents can cancel each other out, forming a zero voltage point at point C, which balances the current on the feeder. The key to the voltage balun is to add a feedback path and build a balanced structure such that the current in the feedback path can cancel out the common-mode current. This principle of the voltage balun has been applied in many studies [11-13].
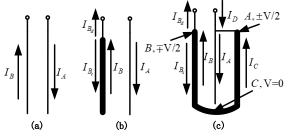

Fig. 4. (a) Balanced transmission line. (b) Unbalanced transmission line. (c) Unbalanced transmission line with a voltage balun.
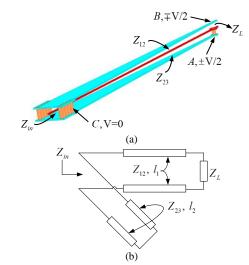

(a)

(b)

Fig. 5. (a) Working principle of the proposed voltage balun. (b) Equivalent circuit of the proposed voltage balun.

However, the SD has strict requirements on the radiated patterns. It is difficult to construct a voltage balun outside the dipole that does not affect these patterns. The voltage balun designed in this communication can be embedded inside the dipole cone and can thus be shielded. Compared with the U-shaped split balun [19], the board width is reduced through multi-layer wiring. Then, a compact, slender balun can be obtained. Fig. 5(a) shows the basic working principle of the designed voltage balun. Points A and B on the two outer conductors are symmetrically located in the structure. Therefore, the voltages at the two points have the same amplitude and opposite phase. Moreover, due to the symmetry of the structure, the voltage at point C (the junction at which the two outer conductors are connected) is always equal to zero. By further connecting the inner conductor to the outer conductor at Point A, the imbalanced voltage at the input is transformed to a pair of balanced voltages at points A and B. With the balanced antenna radiators, the common-mode current flowing on the outer

surface of the outer conductor of the coaxial cable can be ideally eliminated.

Because the balancing effect of the voltage balun comes from the symmetry of the structure, the theoretical bandwidth can be infinitely large. However, the shunt impedance of the parallel stub will limit the bandwidth of the balun. The equivalent circuit of the voltage balun is shown in Fig. 5(b). Here, Z_L represents the load impedance. Z_{12} and Z_{23} represent the equivalent characteristic impedances. l_1 and l_2 represent the lengths of the two transmission lines, and Z_{in} represents the input impedance into the imbalanced port of the balun. It can be shown that

$$Z_{in} = Z_{12} \frac{Z_L + jZ_{12}\tan\beta l_1}{Z_{12} + jZ_L \tan\beta l_1} // jX_p \qquad (1)$$

and

$$jX_p = jZ_{23}\tan\beta l_2 \qquad (2)$$

where $\beta = 2\pi/\lambda_d$, is the wave number, λ_d is the wavelength at the operating frequency. When βl_2 is close to $\pi/2$, jX_p approaches infinity. Then, the input impedance Z_{in} is determined only by the input impedance of the transmission line connected to the load (antenna). To eliminate the effect of the balun on the antenna impedance, the electrical length of the outer conductors is designed to be near a quarter wavelength, with jX_p approaching infinity. Then, due to symmetry, $Z_{in} = Z_L$. In this design, the quarter wavelength can be approximately determined by the following formula:

$$l_2 = \lambda_d / 4 = c / f / \sqrt{\varepsilon_r} = 21.7 \ mm \qquad (3)$$

where c is the speed of light in vacuum and f is the operating frequency (2 GHz). Because l_2 is the length between the middle layer and the bottom layer, the electric field is primarily concentrated in the second core board. The influence of air and the prepreg layer can be ignored. Thus, the relative permittivity ε_r can be considered as approximately equal to that of the core layer ($\varepsilon_r = 3$). The result of equation (3) can be used as an initial value of the design. The optimized value of l_2 is approximately 24.8 mm, which is close to the value calculated from (3).
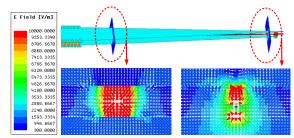

Fig. 6. Electric field distribution in the tapered transmission line.

The top and bottom layers of the voltage balun have the same wiring to maintain the symmetry of the structure. Because the two ends of the balun are respectively connected to the rectangular coaxial and parallel-strip transmission lines, the top conductor adopts a gradual width from wide to narrow, which enables a smooth transition between the coaxial and parallel-strip transmission lines. The tapered balun has both impedance matching and common-mode current suppression functions [20]. As shown in Fig. 6, when the transmission line is narrow, there is a strong electric field distribution both inside and outside the transmission line. When the line is wide, the electric field is mainly concentrated inside the transmission line. At the same time, the current is confined in the transmission line, and the current on the outer surface of the transmission line is very small. Therefore, the common-mode current can be further reduced.

The common-mode current is difficult to quantify. This current can usually be qualitatively determined from the relative current value of the outer surface of the coaxial cable and the symmetry of the pattern. The common-mode current suppression provided by the antenna can be qualitatively expressed by the common-mode current suppression ratio. The common-mode current suppression ratio of the dipole can be approximately expressed by the following formula [21]:

$$R_{CM} = \frac{I_{\max\_dipole}}{I_{\max\_cable}} \qquad (4)$$

where $I_{\max\_dipole}$ and $I_{\max\_cable}$ represent the maximum current on the antenna and on the outer surface of the coaxial cable, respectively. It can be seen from Fig. 7(a) that the common-mode current suppression ratio of the designed dipole obtained from simulation is approximately 20 dB, indicating a good suppression effect. As a comparison, the current distribution of the dipole without a balun is shown in Fig. 7(b). It can be seen that the current on the cable is as large as the current on the radiator, which will obviously affect the radiation pattern.
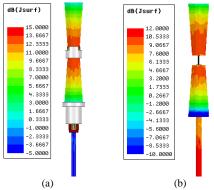

(a)   (b)

Fig. 7. Simulated current distribution at 2 GHz (a) with and (b) without the designed balun.

The vertical patterns obtained under different simulation conditions are compared in Fig. 8. The pattern of the dipole fed by a 500-mm-long cable with the balun is very close to an ideal pattern, indicating that the common-mode current has been well suppressed. In contrast, the pattern of the dipole directly fed by a 500-mm-long cable without the balun has obvious ripples because the common-mode current on the outer surface of the cable affects the radiation. Due to the existence of the common-mode current, the measured results will be greatly affected by the cable length and placement.
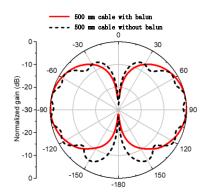
Fig. 8. Simulated vertical radiation patterns with and without the designed balun at 2 GHz.

III. MEASUREMENT AND ANALYSIS

A prototype of the proposed dipole is shown in Fig. 9(a). For comparison, a traditional calibration dipole [22] (shown in Fig. 9(b)) was also measured. The S-parameters of the antenna were measured by a Keysight N5230AC vector network analyzer. The radiation performance was measured in a General Test System Dart-9000 anechoic chamber. The measurement set-up is shown in Fig. 9(c).
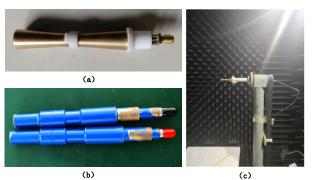

Fig. 9. (a) Photograph of the prototype. (b) A traditional calibration dipole. (c) Measurement set-up in the anechoic chamber.
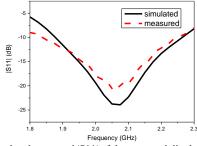

Fig. 10. Simulated and measured |S11| of the proposed dipole.

The simulated and measured $|S_{11}|$ values are shown in Fig. 10 and show good agreement with each other. The measured $|S_{11}|$ has a value below -10 dB for 1.84–2.24 GHz, and the relative bandwidth is close to 20%. The simulated and measured patterns are shown in Fig. 11. It can be seen that the simulation and measurement are in good agreement. The symmetry of the measured vertical pattern is very good, and the maximum gain point does not deviate from the horizontal plane. Based on the patterns, it can be concluded that the designed voltage balun has reached the simulation target and that the common-mode current is well suppressed for a relative bandwidth of

approximately 15% (approximately 1.9–2.2 GHz). The measured results for our design and the traditional dipole are compared in Table II. It can be seen from Fig. 11 and Table II that the proposed antenna has the following advantages over the traditional calibration antenna: greater symmetry in the patterns, no obvious ripples, and a maximum gain point that is closer to the horizontal plane. The measured cross-polarization ratio of the horizontal plane exceeds 27 dB.
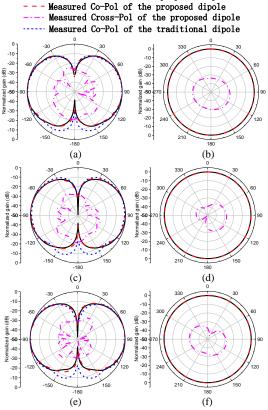

Fig. 11. Simulated and measured patterns of the proposed dipole and measured vertical patterns of a traditional dipole. (a) Vertical plane at 1.9 GHz. (b) Horizontal plane at 1.9 GHz. (c) Vertical plane at 2.05 GHz. (d) Horizontal plane at 2.05 GHz. (e) Vertical plane at 2.2 GHz. (f) Horizontal plane at 2.2 GHz.

TABLE II
COMPARISON OF THIS WORK AND A TRADITIONAL DIPOLE

Antenna	This work			Traditional dipole		
Frequency (GHz)	1.90	2.05	2.20	1.90	2.05	2.20
Maximum gain angle (deg)	90	84	-86	-100	65	82
Difference between maximum gain and horizontal gain (dB)	0	0.23	0.19	0.36	1.24	0.32
Horizontal gain variation (dB)	0.17	0.15	0.11	0.29	0.21	0.11
Peak gain (dBi)	1.86	2.15	2.11	1.46	1.95	1.61
Efficiency (%)	89.3	98.2	86.4	81.8	87.1	86.0
Cross-polarization ratio (dB)	>27	>27	>27	>23	>30	>30
Relative bandwidth (return loss > 10 dB) (%)	15			15		

Fig. 12 shows the simulated and measured horizontal gain ripple, gain and efficiency. The measured gain variation is less than 0.2 dB, which meets the measurement requirements of the Cellular Telecommunications and Internet Association (CTIA) for gain consistency in multi-probe systems [23]. The simulated and measured gains are both approximately 2 dBi, and the

fluctuation of the gain in the designed frequency band is less than 0.5 dB. The maximum gain difference between simulation and measurement is less than 0.15 dB, which is within a reasonable uncertainty of the gain measurement [23]. The measured antenna efficiency is approximately 90% (86.4%~98.2%). Finally, from the detailed comparison in Table II, it can be seen that the proposed antenna can maintain the advantages of a traditional calibration dipole [22], such as a low cross-polarization level and a small horizontal gain variation, while maintaining an enhanced pattern symmetry.
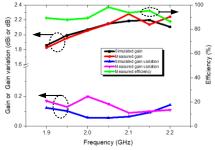

Fig. 12. Simulated and measured gain, gain variation in the horizontal plane and measured efficiency of the proposed dipole.

IV. CONCLUSION

A high-performance SD suitable for antenna calibration has been proposed in this communication. A compact voltage balun combined with a tapered balun using a multi-layer printed circuit board was designed to suppress the common-mode current on the outer surface of the coaxial cable. The voltage balun and feeding network were innovatively embedded inside a dipole cone. The balun is positioned far from the center of the dipole and is as compact as possible for this design. Thus, the balun and the network can achieve the desired functions without affecting the dipole pattern. The measured results show that the antenna can achieve the vertical plane pattern of an SD over a relative bandwidth of 15%. The horizontal plane gain ripple is less than 0.2 dB, and the cross-polarization ratio exceeds 27 dB. The designed antenna provides the two primary features of an SD, i.e., a symmetrical pattern and measurable gain. Thus, this design can be used as a calibration antenna for antenna measurement systems.

REFERENCES

[1] Zhi Ning Chen, Ning Yang, Yong-Xin Guo and M. Y. W. Chia, "An investigation into measurement of handset antennas," *IEEE Trans. Instrum. Meas.*, vol. 54, no. 3, pp. 1100-1110, June 2005.

[2] T. Fukasawa, N. Yoneda and H. Miyashita, "Investigation on current reduction effects of baluns for measurement of a small antenna," *IEEE Trans. Antennas Propag.*, vol. 67, no. 7, pp. 4323-4329, July 2019.

[3] Y. Zheng *et al*., "Calibration loop antenna for multiple probe antenna measurement system," *IEEE Trans. Instrum. Meas.*, vol. 69, no. 8, pp. 5745-5754, Aug. 2020.

[4] L. Chi, Z. Weng, Y. Qi and J. L. Drewniak, "A 60 GHz PCB wideband antenna-in-package for 5G/6G applications," *IEEE Antennas Wireless Propag. Lett.*, doi: 10.1109/LAWP.2020.3006873.

[5] T. Oki, N. Michishita, H. Morishita and M. Sakuma, "Broadband sleeve antennas with a choke," *2015 IEEE International Symposium on Antennas and Propagation & USNC/URSI National Radio Science Meeting*, Vancouver, BC, Canada, 2015, pp. 2007-2008

[6] C. Icheln, J. Krogerus and P. Vainikainen, "Use of balun chokes in small-antenna radiation measurements," *IEEE Trans. Instrum. Meas.*, vol. 53, no. 2, pp. 498-506, April 2004.

[7] J. Jung, J. Cho and S. Kim, "Analysis of sleeve dipole antennas fed by ferrite-loaded coaxial cables for a scaled-down cross-borehole radar," *IEEE Trans. Antennas Propag.*, vol. 65, no. 11, pp. 6130-6133, Nov. 2017.

[8] J. S. McLean, "An alternative experimental determination of a two-port dipolar antenna model," in *IEEE Letters on Electromagnetic Compatibility Practice and Applications*, vol. 2, no. 1, pp. 2-10, March 2020.

[9] C. Icheln, M. Popov, P . V ainikainen, and S. He, "Optimal reduction of the influence of RF feed cables in small antenna measurements,"*Microw. Opt. Tech. Lett.*, vol. 25, pp. 194–196, 2000.

[10] Kraus, John Daniel. Antennas for all applications. Publishing House of Electronics Industry, 2008, pp. 804-812.

[11] L. H. Ye, X. Y. Zhang, Y. Gao and Q. Xue, "Wideband dual-polarized four-folded-dipole antenna array with stable radiation pattern for base-station applications," *IEEE Trans. Antennas Propag.*, vol. 68, no. 6, pp. 4428-4436, June 2020.

[12] C. F. Ding, X. Y. Zhang and M. Yu, "Simple dual-polarized filtering antenna with enhanced bandwidth for base station applications," *IEEE Trans. Antennas Propag.*, vol. 68, no. 6, pp. 4354-4361, June 2020.

[13] L. Chi *et al*., "Rugged linear array for IoT applications," *IEEE Internet Things J.*, vol. 7, no. 6, pp. 5078-5087, June 2020.

[14] T. Rahim, F. A. Abbasi and Jiadong Xu, "Dual band sleeve dipole antenna for WLAN applications," 2016 10th European Conference on Antennas and Propagation (EuCAP), Davos, Switzerland, 2016, pp. 1-3

[15] Zhanghua, Cai , et al. "DC ground compact wideband omnidirectional vertically polarised slot loop antenna for 4G long-term evolution applications." *IET Microw. Antennas Propag.*, vol. 12, no. 7, pp. 1087-1092, July 2018.

[16] D. Chang and C. Chen, "The performance comparison of the sleeve antenna and the array sleeve antenna," 2010 International Conference on Applications of Electromagnetism and Student Innovation Competition Awards (AEM2C), Taipei, Taiwan, 2010, pp. 112-116

[17] S. Jung, T. Jung and J. Woo, "Design of sleeve dipole antenna for suppressing leakage current on a coaxial cable," *IEEE Antennas Wireless Propag. Lett.*, vol. 13, pp. 459-462, 2014.

[18] Seo-Cheol Jung, Yoon-Seon Choi and Jong-Myung Woo, "Small sleeve dipole antenna using inner short stub," *2014 20th International Conference on Microwaves, Radar and Wireless Communications (MIKON)*, Gdansk, Poland, 2014, pp. 1-3

[19] R. Li, T. Wu, B. Pan, K. Lim, J. Laskar and M. M. Tentzeris, "Equivalent-circuit analysis of a broadband printed dipole with adjusted integrated balun and an array for base station applications," *IEEE Trans. Antennas Propag.*, vol. 57, no. 7, pp. 2180-2184, July 2009.

[20] J. W. Duncan and V. P. Minerva, "100:1 bandwidth balun transformer," *Proc. IRE*, vol. 48, no. 2, pp. 156-164, Feb. 1960.

[21] Y. Zheng, Y. Qi, F. Li and W. Wang, "Research on common mode current aspect of multi-probe antenna measurement system," *Chinese Journal of Scientific Instrument*, vol. 41, no. 9, pp. 140-150, Sep. 2020.

[22] Electric Sleeve Dipoles, Microwave Vision Group, France [Online]. Available: https://www.mvg-world.com/en/products/antennas/reference-antennas/electric-sleeve-dipoles.

[23] Telecommunications and Internet Association, "Test plan for 2 × 2 downlink MIMO and transmit diversity over-the-air performance," Revision 1.1, Aug. 2016.